PROCEEDINGS OF SCIENCE

# Non-WIMP dark matter searches with the ATLAS detector

**Peter Krämer[a,*] on behalf of the ATLAS collaboration**

[a] *Johannes Gutenberg Universität, Staudingerweg 7, Mainz, Deutschland*

*E-mail:* peter.kramer@cern.ch

Collider searches for dark matter (DM) so far have mostly focused on scenarios where DM particles are produced in association with heavy Standard Model (SM) particles or jets. However, no deviations from SM predictions have been observed. Several recent phenomenology papers have proposed models that explore the possibility of accessing the strongly-coupled dark sector, giving rise to unusual and unexplored collider topologies. The results of recent searches for dark QCD, semi-visible jets, dark sector particles, dark photons, LLPs, and ALPs with 13 TeV pp data from the LHC, their interplay and interpretation will be presented.

*XVIII International Conference on Topics in Astroparticle and Underground Physics (TAUP2023)*
*28.08_01.09.2023*
*University of Vienna*

*Speaker





PoS(TAUP2023)068

## 1. Introduction

Many experimental results show large evidence for dark matter. This article presents three searches performed on data recorded by the ATLAS detector at the Large Hadron Collider (LHC) at CERN. In the first part, dark matter candidates interacting similarly to the quarks in the Standard Model (SM) are discussed. The second part treats Axion-Like Particles (ALPs), which could be a dark matter candidate but could also explain other long-standing problems in physics such as the $(\mathrm{g}-2)_\mu$ discrepancy.

## 2. Dark showers

Several theoretical models propose a strongly coupled dark sector. Such a dark sector could lead to different, yet unexplored, detector signatures. One of those features could be so-called ´dark showers´, which, similarly to SM showers, consist of dark quarks hadronizing into dark mesons. Some of these hadrons could decay back to SM particles, while others could be stable or long-lived. Depending on those properties different detector signatures are possible.

If all of the dark hadrons decay back to SM particles promptly, they would form a jet with more tracks and a larger radius. These jets are called ´dark jets´.

If only a fraction of the dark hadrons decay back to SM particles within the active detector volume, it will lead to a jet aligned with some missing transverse energy ($E_\mathrm{T}^\mathrm{miss}$). These signatures are called ´semi-visible jets´.

Some of the dark hadrons could also have a lifetime that could lead to a decay to SM particles only in the outer layers of the detector. In that case, the standard reconstruction algorithms are not able to catch these ´emerging jets´ and special methods are needed.

### 2.1 Dark quarks in di-jet

This section summarizes a search for resonant production of dark quarks in a di-jet final state [1]. This analysis aims to search for a dark quark anti-quark pair produced via a Z´ resonance in a di-jet spectrum. Large radius jets in the $\mathrm{p_T}$-range between 500 GeV and 3 TeV for the highest energetic jet and a range between 400 GeV and 3 TeV for the 2$^{\mathrm{nd}}$ highest respectively, are selected. The background is reduced by requiring an additional selection on the number of tracks within the jets. The $n_\mathrm{track}$distributions for the two hardest jets are shown in Figure 1.

It can be seen that the number of tracks for signal is expected to be higher than in SM-like jets. However, $n_\mathrm{track}$ is also correlated to the $\mathrm{p_T}$ of the jet and applying a simple cut on it would sculpt the di-jet distribution. To avoid this, a new observable $n^\epsilon_\mathrm{track}$ is defined such that a target efficiency $\epsilon = 1\%$ for background events is reached. The number of tracks is evaluated for the (sub)leading jet in bins of $m_\mathrm{JJ}$individually and then fitted over the whole mass range getting the minimal value $\mathrm{P}_{J_i}$ leading to the target efficiency with respect to $m_\mathrm{JJ}$. These are evaluated for each jet such that $n^\epsilon_\mathrm{track} = n_\mathrm{track} - \mathrm{P}_{J_i} > 0$ holds true. By requiring this for both jets, the signal efficiency drops to 1-28% depending on the signal model and the background is reduced by approximately 99.99%. A control region enhanced in multi-jet background is deployed by inverting the $n^\epsilon_\mathrm{track}$ criterion. The shape of the background is taken from this CR, while the normalization is left as a free parameter in the final fit. In the $m_\mathrm{JJ}$ spectrum, a bumphunter [2] search is performed. The spectrum with the

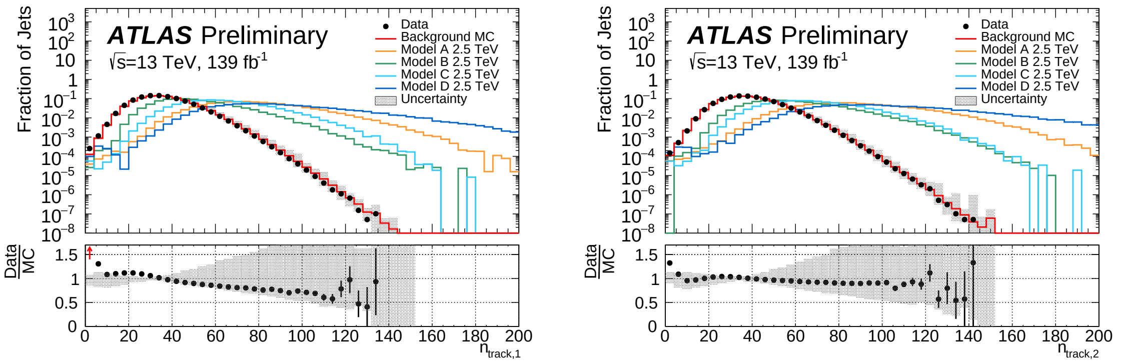


**(a)** **(b)**

**Figure 1:** Number of tracks within the jet with most (a) and second most (b) $p_T$ for data, background and several signal models [1].

results of the bumphunter search are shown in Figure 2 (a). The most promising region is between 1500 and 1700 GeV with a local $p_0$ value of 0.63. Over all, no significant excess can be seen and upper limits on different signal models can be set. This can be seen in Figure 2 (b) for one model. It can be seen that this model can be excluded up to a $Z'$ mass around 3 TeV.

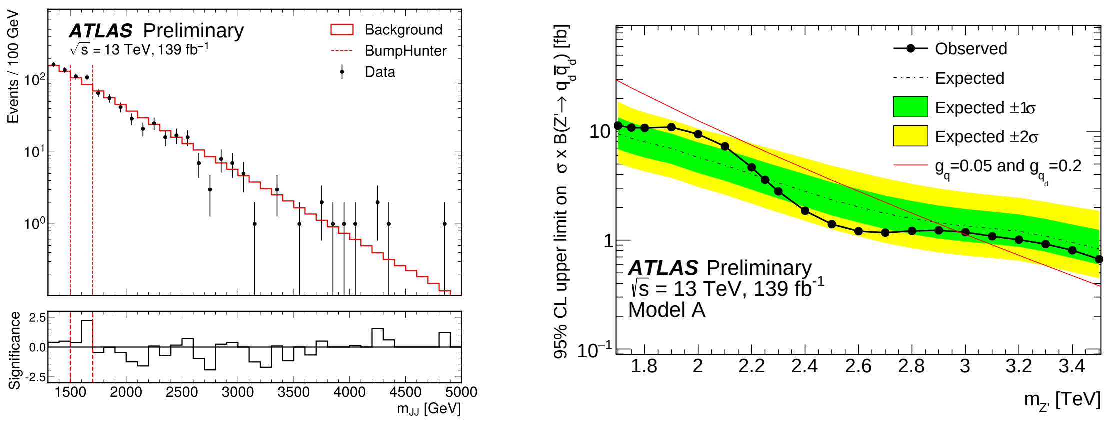


**(a)** **(b)**

**Figure 2:** Invariant mass distribution of the di-jet spectrum with the most promising region of the bumphunter search between the vertical red lines (a) and upper limits on the branching ratio in terms of $m_{Z'}$ (b) [1].

## 2.2 Non-resonant, semi-visible jets

In this section, the search for non-resonant production of semi-visible jets with the ATLAS detector [3] is summarized. First, events are selected with $E_T^{miss} > 200$ GeV and at least two jets with one being aligned within $\Delta\phi < 2.0$ of the $E_T^{miss}$ direction. The signal region (SR) is defined with $E_T^{miss} > 600$ GeV and a scalar sum of $p_T$ of jets $H_T > 600$ GeV. No electrons or muons with $p_T > 7$ GeV are allowed in the SR. Different control regions (CR) are defined to constrain the background contributions. The 1L CR requires exactly one muon and no b-tagged jet and W+jet events are enhanced in this phase space. The 1L1B CR is enhanced with semileptonic $t\bar{t}$, single-top-quark and W+heavy-flavor jet events by requiring one muon and one b-tagged jet. Finally the 2L CR has two oppositely charged muons with an invariant mass between 66 GeV and 116 GeV and no b-tagged jet and is dominated by Z+jets events.

Both the SR and CRs are further split into 9 bins of two mostly uncorrelated variables, which are $\mathrm{p_T}$ balance: $p_{\mathrm{T}}^{\mathrm{bal}} = \frac{|p_{\mathrm{T}}(\vec{j}_1)+p_{\mathrm{T}}(\vec{j}_2)|}{|p_{\mathrm{T}}(\vec{j}_1)|+|p_{\mathrm{T}}(\vec{j}_2)|}$ and azimuthal separation: $|\phi_{max} - \phi_{min}|$. A binned maximum-likelihood fit is performed simultaneously in the four regions to constrain both signal and background contributions. The post-fit distribution of the SR can be seen in Figure 3 (a). No excess is found and 95% CL upper limits are set on the mediator mass $\mathrm{m}_\phi$ and the fraction of stable dark hadrons in the jet $\mathrm{R_{inv}}$. These exclusion limits can be seen in Figure 3 (b) depicted as a red line. In blue, exclusion limits of a previous mono-jet search are shown [4].

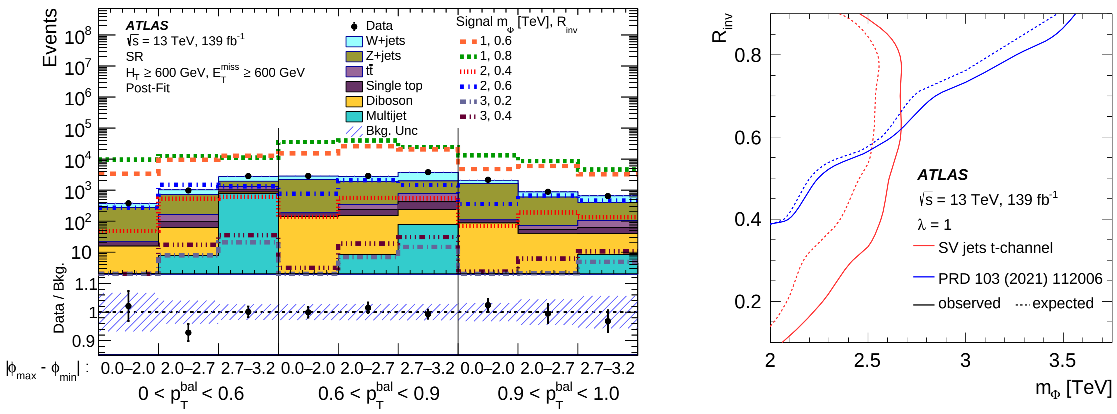


**(a)** **(b)**

**Figure 3:** Post-fit distribution in the SR (a) and exclusion limits with respect to $\mathrm{m}_\phi$ and $\mathrm{R_{inv}}$ (b) [4].

## 3. Anomalous H→ $aa$ → $\gamma\gamma\gamma\gamma$ decays

This section summarizes the search for ALPs in exotic Higgs decays with a four photon final state (H→ $aa$ → $\gamma\gamma\gamma\gamma$)[5]. This analysis searches for ALPs with masses between 100 MeV and 62 GeV and ALP-photon couplings between $10^{-5}$ and 1. This large parameter space results in differences in the event kinematics. If the ALP is very light (< 3.5 GeV) it gets a large boost from the Higgs boson decay and the decay photons appear collimated and are dominantly reconstructed as a single photon object. To distinguish these from photon objects that stem from a single photon, e.g. in H→ $\gamma\gamma$ events, neural networks are developed. If the coupling $\mathrm{C}_{a\gamma\gamma}$ is small, the ALPs have a significant lifetime which leads to displaced decays of the ALP. By applying custom systematic uncertainties, this analysis is sensitive to ALP decays with a displacement up to 1970mm in the x-y-plane.

After applying some preselections on the kinematic properties of the photons, all events are classified in one of five categories, which are: 4 Single (4S), 3 Single (3S), 2 Merged (2M), 1

Merged 1 Single (1M1S) and 2 Single (2S). For events with three or four photons, a neural network is used to select the correct combination of photons that belong to the same ALP. This enables a mass reconstruction and a consequent splitting of the 3S and 4S category into four $m_a$ bins.

The continuous background is estimated from data by a sideband fitting method in the invariant photon mass spectrum ($m_{inv}^{reco}$) in each category. The background estimation in the 4S category for ALP masses between 25 GeV and 40 GeV is shown in Figure 4 (a). In the two photon categories, the $H \to \gamma\gamma$ background contribution is estimated from simulation. Signal distributions for different $m_a/C_{a\gamma\gamma}$-pairs are also simulated. Each pair is fitted simultaneously in the two most sensitive categories using a binned maximum-likelihood method. The most sensitive categories are 2M and 1M1S for $m_a < 3.5$ GeV and 3S+4S for higher masses. Upper limits on $\mathcal{B}(H \to aa \to \gamma\gamma\gamma\gamma)$ are derived using the $CL_S$-method. Upper limits for the coupling $C_{a\gamma\gamma} = 0.01$ are shown in Figure 4 (b). These upper limits can be transformed to exclusion limits in the $m_a/C_{a\gamma\gamma}$-plane. This is depicted in Figure 4 (c).

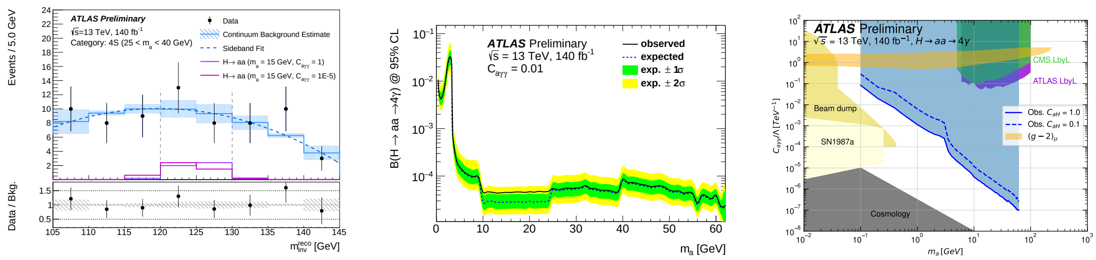


(a) (b) (c)

**Figure 4:** Continuous background in the $m_{inv}^{reco}$-spectrum of the 4S category with 25 GeV $< m_a <$ 40 GeV with sideband-fit (a). Upper limits on $\mathcal{B}(H \to aa \to \gamma\gamma\gamma\gamma)$ for $C_{a\gamma\gamma} = 0.01$ (b) and 2D exclusion limits (c) [5].



## References

[1] ATLAS Collaboration. Search for Resonant Production of Dark Quarks in the Di-jet Final State with the ATLAS Detector. Technical report, CERN, Geneva, 2023. All figures including auxiliary figures are available at ATLAS-CONF-2023-047.

[2] Georgios Choudalakis. On hypothesis testing, trials factor, hypertests and the BumpHunter. In *PHYSTAT 2011*, 1 2011.

[3] ATLAS Collaboration. Search for non-resonant production of semi-visible jets using run 2 data in atlas. *Physics Letters B*, 848:138324, 2024.

[4] ATLAS Collaboration. Search for new phenomena in events with an energetic jet and missing transverse momentum in $pp$ collisions at $\sqrt{s} = 13$ TeV with the ATLAS detector. *Phys. Rev. D*, 103:112006, Jun 2021.

[5] ATLAS Collaboration. Search for short- and long-lived axion-like particles in $H \to aa \to 4\gamma$ decays with the ATLAS experiment at the LHC. Technical report, CERN, Geneva, 2023. All figures including auxiliary figures are available at ATLAS-CONF-2023-040.